Proceedings of the
5th European Conference on Microfluidics – µFlu18
3rd European Conference on Non-Equilibrium Gas Flows – NEGF18
February 28-March 2, 2018 – Strasbourg, France

µFLU-NEGF18-140

IMPACT OF SURFACTANT ON THE DRAG REDUCTION POTENTIAL OF SUPERHYDROPHOBIC SURFACES

François J. Peaudecerf[1], Julien R. Landel*[2], Raymond E. Goldstein[3]
Paolo Luzzatto-Fegiz[4]
[1]ETH Zürich, Institut für Umweltingenieurwissenschaften, 8093 Zürich, Switzerland
peaudecerf@ifu.baug.ethz.ch
[2]School of Mathematics, University of Manchester, Manchester, M13 9PL, UK
julien.landel@manchester.ac.uk
[3]Department of Applied Mathematics and Theoretical Physics, Centre for Mathematical Sciences, University of Cambridge, Cambridge, CB3 0WA, UK
reg53@cam.ac.uk
[4]Department of Mechanical Engineering, University of California, Santa Barbara, CA 93106 USA
fegiz@engineering.ucsb.edu

KEY WORDS

Superhydrophobic surface, drag reduction, surfactant, Marangoni stress, plastron.

SHORT SUMMARY

Superhydrophobic surfaces (SHSs) can potentially achieve drag reduction for both internal and external flow applications. However, experiments have provided inconsistent results, with many studies reporting significantly decreased performance. While a complete explanation is yet to be found, it has been proposed that surfactants, ubiquitous in flow applications, could be responsible, as Marangoni stresses could develop when the edges of the SHS are not aligned with the flow. However, testing this hypothesis has been challenging. Even careful experiments with purified water have shown large interfacial stresses. We address this question with surfactant-inclusive numerical simulations and experiments in a microchannel. By imposing a time-dependent pressure gradient, we are able to drive complex interface dynamics that can only be explained by surfactant gradients. Our results demonstrate the role of surfactants in increasing drag over SHSs.

EXTENDED ABSTRACT

Introduction

Superhydrophobic surfaces (SHSs) can reduce drag at solid-liquid interfaces [1]. This is attractive for many applications ranging from maritime transport to pipe flow [1]. In the past 20 years, experiments have shown inconsistent results with some studies achieving significant drag reduction [2-4], whilst others measure negligible drag reduction [5-7]. By contrast, theoretical and numerical models predict large drag reduction and slip velocities [8-9].
Recent studies have suggested that surfactant could be responsible for the reduced performance observed in some experiments [10,11]. Surfactants, naturally present in our environment [12], can

* Corresponding author

induce Marangoni stresses if their concentration varies along the interface. In a recent article [13], we tested this hypothesis experimentally and numerically, considering simple internal Stokes flow over SHSs. We summarize here the main findings of this study, and present preliminary new results for unsteady numerical simulations of SHS flow inclusive of surfactants. We discuss the impact for applications and possible mitigation strategies.

Experimental and numerical results for steady forcing experiments

Using micro particle image velocimetry, we measured the velocity field of gravity driven flows in one-sided SHS microchannels. The microchannels were made of PDMS with the SHS consisting of lanes aligned with the flow. The velocity was measured at different planes away from the SHS (in colour in Fig. 1). The experiments were conducted using purified water (Millipore MilliQ). No surfactant was introduced in these experiments. Temperature was maintained uniform to avoid thermal Marangoni stresses. The hydrostatic pressure was controlled to maintain flat plastrons (≤ 2 microns deflection).

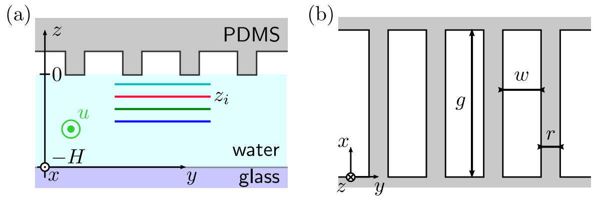

Figure 1: SHS microchannel: (a) longitudinal cross-section; (b) view from below of SHS top surface.

Fig. 2 shows experimental results at constant pressure gradient and for lane lengths: $g = 2\,\text{mm}$ (a), 30 mm (b). No significant slip is found for $g = 2\,\text{mm}$, whereas some slip is found for $g = 30\,\text{mm}$.

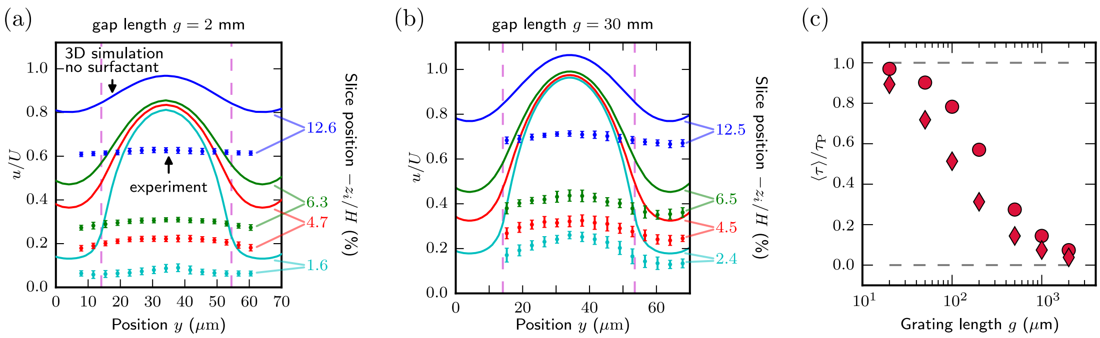

Figure 2: Profile of the normalised experimental velocity (dots) at several distances from the SHS, for lane width $w = 40$ microns, ridge width $r = 20$ microns, and lane length $g = 2\,\text{mm}$ (a) and $g = 30\,\text{mm}$ (b). 3D numerical results for the same conditions and assuming no surfactant are plotted with solid lines. (c) Normalised interfacial stress computed in 2D numerical simulations inclusive of surfactant (concentration $10^{-2}\,\text{mM}$) for varying g (circles) compared to the clean case (diamonds).

The experimental results are consistent with 2D COMSOL numerical simulations (Fig. 2c). These simulations solve the steady Navier-Stokes equations in the bulk, coupled with the transport equations for surfactant in the bulk and at the interface. A modified Frumkin kinetics scheme models the flux of surfactant from the bulk to the interface. The properties of surfactant sodium dodecyl sulfate (SDS) are used. Viscous and Marangoni stresses are coupled at the plastron. We can see in Fig. 2(c) that surfactant-inclusive simulations show a significant increase in interfacial stress for lanes of length 0.01 mm to 1 mm. Wall viscous stress dominates for $g \leq 0.01\,\text{mm}$, whilst Marangoni stresses are too weak for $g \geq 1\,\text{mm}$ due to a reduced surfactant gradient. Although these results are dependent on the actual surfactant concentration and surfactant type, they describe qualitatively the behaviour which can be expected when surfactants are present near the plastron of SHSs. In addition, we tested numerically the influence of surfactant concentration for lanes of 0.1 mm in length. The transition from a free slip interface to a no slip interface occurs between 10^{-4} and 10^{-2} mM. These results are obtained for SDS, which is a mild surfactant. Therefore, most surfactants would produce significant Marangoni stresses, leading to immobilisation of the plastron, at potentially lower concentrations or for longer lane lengths.

Experimental and numerical results for unsteady forcing experiments

We also performed a series of experiments with 30 mm long lanes using a similar setup and protocol as described above. The key difference is that we stopped the flow abruptly after four minutes. The velocity field of a typical experiments measured before and after stopping the flow are shown in Fig. 3(a). Above the ridge, the velocity vanishes immediately after stopping the flow, as expected in Stokes flow regime. However, the velocity field measured above the lanes shows a reverse flow with negative velocity. The peak of the return flow is found just after stopping the flow. The magnitude of the return flow decreases slowly, vanishing after approximately one minute.

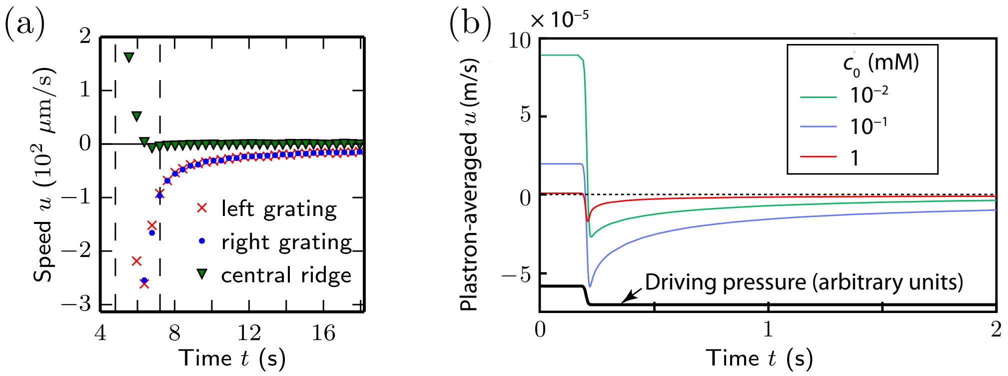

Figure 3: (a) Experimental velocity measured above the plastron and the ridge before and after the background pressure gradient is stopped ($t \approx 5$ s). (b) Results of preliminary 2D numerical simulations, which qualitatively reproduce the unsteady experiments. The flow is stopped at $t \approx 0.25$ s.

This return flow was also observed in unsteady two-dimensional numerical simulations, where the flow was similarly stopped after reaching steady state, as shown in Fig. 3(b). The magnitude of the (positive) loading flow velocity decreases with increasing background concentration of surfactants, owing to an increase in Marangoni stress. However, the magnitude of the peak of the (negative) return flow velocity appears to depend in a non-monotonic fashion with surfactant concentration, with the maximum peak return flow velocity found at intermediate surfactant concentrations. This is probably due to complex nonlinear surfactant dynamics.
The return flow is characteristic of surfactant-driven Marangoni flows. As the pressure gradient initially imposes a flow in the chamber, surfactants adsorbed onto the interface are advected towards the downstream stagnation point of the plastron. At steady state, a gradient of surfactant along the plastron leads to a Marangoni stress that immobilizes the interface. When the background pressure gradient is stopped, the Marangoni stress is no longer opposed, which induces the return flow to recover a uniform concentration of surfactant.

Conclusion

Our numerical and experimental results show that small traces of surfactant can immobilize the plastron. This effect is due to an accumulation of surfactant at the downstream stagnation points

of the air–water interface. Surfactant traces in our experiments, and potentially in previous studies showing reduced slip performance, could originate from unavoidable environmental impurities or uncrosslinked PDMS chains [14]. Interestingly, a past study that achieved very large slip lengths, in agreement with surfactant-free theory, employed annular ridges in a rheometer [3]. Since an annular ridge does not offer stagnation points for surfactant accumulation, it corresponds essentially to infinitely long lanes where Marangoni stresses cannot form. These previous results are therefore consistent with the surfactant hypothesis and our conclusions presented here.
As surfactants are ubiquitous in oceans and rivers, drag reduction by SHS can be strongly impaired. In order to prevent the establishment of adverse surfactant-induced Marangoni stresses, we have shown that increasing the distance between stagnation points can reduce the Marangoni stresses. Our results suggest that lanes longer than $\sim 10\,\mathrm{mm}$ are necessary. We note however that longer lanes tend to have less stable plastron. Furthermore, they require a high degree of control over the manufacturing process, which may not be practical or economical in large-scale applications.

Acknowledgements

We acknowledge financial support from the Raymond and Beverly Sackler Foundation, the Engineering and Physical Sciences Research Council, the European Research Council Grant 247333, Mines ParisTech, the Schlumberger Chair Fund, the UC Santa Barbara Senate and CNSI Challenge Grant, as well as from Churchill and Magdalene Colleges, Cambridge.

References and Citations

[1] Rothstein, J. P. (2010). Slip on superhydrophobic surfaces. *Ann. Rev. Fluid Mech.*, **42**, 89-109.
[2] Ou, J., Perot, B. & Rothstein, J. P. (2006). Laminar drag reduction in microchannels using ultrahydrophobic surfaces. *Phys. Fluids*, **16**, 4635-4643.
[3] Lee, C., Choi, C. H. & Kim, C. J. (2008). Structured surfaces for a giant liquid slip. *Phys. Rev. Lett.*, **101**, 064501.
[4] Jung, Y. C. & Bushan, B. (2010). Biomimetic structures for fluid drag reduction in laminar and turbulent flows. *J. Phys. Condens. Matter*, **22**, 035104.
[5] Lee, C., Choi, C. H. & Kim, C. J. (2016). Superhydrophobic drag reduction in laminar flows: A critical review. *Exp. Fluids*, **57**, 176.
[6] Watanabe, K. Udagawa, Y. & Udagawa, H. (1999). Drag reduction of Newtonian fluid in a circular pipe with a highly water-repelent wall. *J. Fluid Mech.*, **381**, 225-238.
[7] Zhao, J. Du, X. & Shi, X. (2007). Experimental research on friction-reduction with superhydrophobic surfaces. *J. Mar. Sci. Appl.*, **6**, 58-61.
[8] Philip, J. R. (1972). Flows satisfying mixed no-slip and no-shear conditions. *Z. Angew. Math. Physik*, **23**, 353-372.
[9] Lauga, E. & Stone, H. A. (2003). Effective slip in pressure-driven Stokes flow. *J. Fluid Mech.*, **489**, 55-77.
[10] Bolognesi, G., Cottin-Bizonne, C. & Pirat, C. (2014). Evidence of slippage breakdown for a superhydrophobic microchannel. *Phys. Fluids*, **26**, 082004.
[11] Schäffel, D., Koynov, K., Vollmer, D. & Butt, H. J. (2016). Local Flow Field and Slip Length of Superhydrophobic Surfaces. *Phys. Rev. Lett.*, **116**, 134501.
[12] Lewis, M. A. (1991). Chronic and sublethal toxicities of surfactants to aquatic animals: A review and risk assessment. *Water Res.*, **25**, 101-113.
[13] Peaudecerf, F. J., Landel, J. R., Goldstein, R. E. & Luzzatto-Fegiz, P. (2017). Traces of Surfactants can severely limit the drag reduction of superhydrophobic surfaces. *Proc. Natl Acad. Sci. USA*, **114**, 7254-7259.
[14] Hourlier-Fargette, A., Antkowiak, A., Chateauminois, A. & Neukirch, S. (2017). Role of uncrosslinked chains in droplets dynamics on silicone elastomers. *Soft Matt.*, **13**, 3484-3491.